Phytopathology Research

RESEARCH

Open Access

Rice stripe mosaic virus encoded phosphoprotein forms viral factory-like granules and is crucial for viral replication

Zhiyi Wang[1,2], Jingyi Zhang[1], Xinyue Song[1], Siping Chen[1], Xue Cao[1], Xin Yang[1], Guohui Zhou[1*] and Tong Zhang[1,2*]

Abstract

Viral proteins can aggregate into granules within host cells, known as viral factories, or viroplasms, which play a pivotal role in facilitating viral replication and shielding the viral genome from cellular defense mechanisms. Rice stripe mosaic virus (RSMV), a plant cytorhabdovirus, is notorious for causing significant damage to rice production. Despite its impact, the mechanisms underlying the replication and assembly of RSMV remain largely unexplored. In this investigation, we established a minireplicon (MR) system of RSMV in *Nicotiana benthamiana* plants to assess the influence of RSMV phosphoprotein (P) on viral replication. Our findings indicate that RSMV P forms viral factory-like granules and is an important component of viral factories. Further investigation showed that the formation of P granules is indispensable for MR replication. Through deletion analysis, we identified the IDR2 region of P as crucial for granule formation and MR replication. These findings underscore the necessity of P protein granule formation in viral replication.

Keywords Rice stripe mosaic virus, Reverse genetics system, Mini-replicon, Phosphoprotein, Rhabdovirus

Background

The viral reverse genetics system is a crucial tool for studying viral protein functions and pathogenic mechanisms. Given that the positive-sense RNA viral genome can serve as mRNA and is infectious, most infectious clones of positive-sense RNA viruses have been successfully constructed (Ahlquist et al. 1984; Damayanti et al. 1999; Nayaka et al. 2023). However, compared with positive-sense RNA viruses, progress in research on the reverse genetics of negative-sense RNA viruses is relatively slow. The minimal infectious and replicating unit of negative-sense RNA (NSR) viruses is the viral ribonucleoprotein (RNP), rather than the naked viral genomic RNA. It plays a crucial role in the replication and transcription of the viral genome (Luytjes et al. 1989; Pattnaik et al. 1991; Ganesan et al. 2013). Since the majority of negative-sense viral genomes are quite long, studying them can be challenging. Therefore, it is necessary to use a reverse genetic system, such as a minireplicon (MR), to explore and optimize experimental conditions before constructing a full-length infectious clone for viral rescue (Rose 1996; Luytjes et al. 1989).

In 1994, rabies virus (RABV) was rescued from a full-length cDNA clone, marking the true establishment of the reverse genetics system for negative-sense RNA viruses (Conzelmann et al. 1994; Schnell et al. 1994).

*Correspondence:
Guohui Zhou
ghzhou@scau.edu.cn
Tong Zhang
zhangtong@scau.edu.cn
[1] Guangdong Province Key Laboratory of Microbial Signals and Disease Control, College of Plant Protection, South China Agricultural University, Guangzhou 510642, China
[2] State Key Laboratory of Green Pesticide, South China Agricultural University, Guangzhou 510642, China

As technology continues to mature, reverse genetics systems have been established for several plant NSR viruses. The first such virus was sonchus yellow net virus (SYNV), a member of the *Alphanucleorhabdovirus* genus (Wang et al. 2015). Subsequently, a reverse genetics system for the cytorhabdovirus, barley yellow striate mosaic virus (BYSMV) was successfully established in *Nicotiana benthamiana* and barley (Gao et al. 2019). The research on segmented negative-sense RNA viruses had also achieved a breakthrough, as such a system was established for the orthotospovirus tomato spotted wilt virus (TSWV), with three genomic RNA segments (Feng et al. 2019). In addition, lettuce necrotic yellows virus (LNYV), a member of the genus *Cytorhabdovirus*, and rice stripe virus (RSV), a member of the genus *Tenuivirus*, have MR systems successfully constructed (Ibrahim et al. 2020; Feng et al. 2021). These systems have greatly advanced the study of NSR viruses.

Multiple studies have shown that viral proteins can form granules (also known as inclusion bodies) within host cells, which have been demonstrated to be viral replication-related structures (Netherton et al. 2011; Novoa et al. 2005). The genome structure of viruses in the family *Rhabdoviridae* is relatively conserved (Dietzgen et al. 2016). Studies on RABV have shown that the P protein has a specific sequence that binds to the N and L proteins, playing a crucial role in the viral transcription and replication processes (Nikolic et al. 2019; Mavrakis et al. 2003; Castel et al. 2009; Chenik et al. 1998). The N-terminal domain (P^{NTD}) of the RABV P protein (1–22 aa) can bind to the RNA polymerase L and N^0 (the soluble form of the N protein devoid of RNA) (Mavrakis et al. 2003). Additionally, the C-terminal domain of the P protein (P^{CTD}) interacts with RNA-bound N protein. The P protein also contains two central disordered regions (IDD1 and IDD2) flanking a dimerization domain (91–132 aa) (Nikolic et al. 2019; Gérard et al. 2009). The P proteins of barley yellow striate mosaic virus (BYSMV) and northern cereal mosaic virus (NCMV) form granules in vivo when their N-terminus is fused with GFP fluorescence, but fusion at the C-terminus disrupts the punctate localization of the P protein (Fang et al. 2019). Research on the function of the BYSMV P protein has revealed that the formation of granules is crucial for virus replication. Furthermore, the P protein acts as a bridge, pulling the genomic RNA, N protein, and L protein into the aggregates to form replication centers (Fang et al. 2019). These studies emphasized the multifunctional nature of the P protein, which is crucial for viral transcription and replication.

Rice stripe mosaic virus (RSMV) is a newly discovered cytorhabdovirus and is transmitted persistently by the leafhopper *Recilia dorsalis* (Yang et al. 2017a, b). The RSMV genome is a single negative-sense RNA with a length of 12,774 nt. Its complementary strand contains seven non-overlapping open reading frames (ORFs), which encode seven proteins in the following order: nucleocapsid protein (N), phosphoprotein (P), non-structural protein P3, matrix protein (M), glycoprotein (G), non-structural protein P6 and polymerase protein (L) (Yang et al. 2017a; Wang et al. 2021). In this study, two minireplicon (MR) systems were constructed based on the RSMV genome and the anti-genome sequence (RSMV-gMR/agMR). After injecting these systems into *Nicotiana benthamiana*, the expression of reporter genes was successfully detected, indicating that both MR systems were functioning properly. Additionally, this study utilized the agMR system to investigate the role of RSMV P protein granules in virus replication. The results initially suggested that RSMV P is an important component for viral factories. Furthermore, these findings demonstrate that the formation of P protein granules is crucial for virus replication.

Results

Engineering the RSMV anti-genomic and genomic RNA minireplicon system in *N. benthamiana* leaves

Based on the RSMV anti-genomic RNA, we generated RSMV anti-genomic minireplicons (agMRs), which contained an EGFP and mRFP reporter gene substituted for the viral *N* and *P* genes, respectively. RSMV genomic minireplicons (gMRs) contained identical sequences but in an inverted orientation with the previously engineered anti-genomic RNA (agRNA) transcriptionplasmid agMR (Fig. 1a). The genes of core proteins N, P, and L were engineered into pGD vectors for expression, respectively (Fig. 1a). The genes of three viral suppressors of RNA silencing (VSRs), including tomato bushy stunt virus p19, tobacco etch virus HC-Pro, and barley stripe mosaic virus γb, were combined into one plasmid (Fig. 1a).

To assess the agMR and gMR systems, *Agrobacterium tumefaciens* harboring agMR/gMR and plasmids for expression of the RSMV N, P, and L proteins and the VSRs were mixed and coinfiltrated into *N. benthamiana* leaves. At 12 days post-infiltration (dpi), both the agMR and gMR systems showed GFP expression throughout the infiltrated leaves under ultraviolet light (UV) (Fig. 1b). Confocal fluorescence microscopy was used to test GFP and RFP expression, and the results showed that approximately 40% of cells showed GFP and RFP foci in both the agMR- and gMR-expressing leaves, respectively(Fig. 1c, d). Quantitative RT-PCR (qRT-PCR) analysis was performed to determine the agMR/gMR replication in the levels. The full-length MR RNA abundance, representative of MR replication, was tenfold higher in the agMR system than in the gMR system at

12 dpi (Fig. 1e). Taken together, we have established an RSMV agMR and gMR system in *N. benthamiana* leaves.

The N, P, L, and VSRs are required for agMR/gMR reporter gene expression

To initiate the expression of agMR reporter genes, the coexpressed N, P, and L core proteins assemble in vivo at the 5' termini of the nascent viral agRNAs to produce active anti-genomic nucleocapsids (agNCs). The agNCs then initiate replication of gRNAs, which assemble with the core proteins to generate gNCs capable of transcribing reporter gene mRNAs (Ganesan et al. 2013).

To determine the individual N, P, L, and VSR protein requirement for reporter gene expression, Agrobacterium mixtures were tested in *N. benthamiana* leaves in the absence of N, P, L, agMR/gMR, or VSRs, respectively. GFP expression was first detected under UV light, and every Agrobacterium combination showed GFP foci throughout the infiltrated leaves. This indicates that the reporter gene GFP can still be expressed, without the presence of N, P, L, and VSR proteins (Fig. 2a). Confocal fluorescence microscope observations showed that the GFP fluorescence intensity was significantly higher in the complete combination of the agMR/gMR system than in any other combinations (Fig. 2b, c). Meanwhile, the second reporter gene, mRFP, was only observed in the complete combination of the agMR/gMR system (Fig. 2b, c). In agreement with the results shown in confocal fluorescence observations, Western blotting analyses further indicated that residual GFP accumulated in leaves without the expression of N, P, or L proteins, resulting from direct translation from the GFP ORF at the 5'end of the agRNA transcripts. However, RFP at the second ORF was absolutely reliant on the co-expression of the complete combination (Fig. 2d, e). These results showed that all components are essential for agMR/gMR reporter gene expression in vivo.

The RSMV GFP-P forms VF-like granules and is functional for agMR replication

We next investigated the subcellular localization of the core proteins N and P, respectively. The N and P protein genes were fused to the coding sequences of N or C termini of GFP under the control of the cauliflower mosaic virus (CaMV) 35S promoter (Additional file 1: Fig S1a and Fig. 3a). Agrobacterium harboring plasmids for expression of GFP-tagged proteins were infiltrated into H2B-RFP transgenic *N. benthamiana* plants. Confocal fluorescence microscopy showed that both N-GFP and GFP-N were localized in the cytoplasm, but not in the nuclei (Additional file 1: Figure S1b). On the contrary, GFP-P formed granule in the cytoplasm, which are usually thought of as viral factory (VF)-like granules (Fig. 3b). Meanwhile, P-GFP mostly localized in the cytoplasm and formed very small VF-like granules (Fig. 3b). To determine whether RSMV P is involved in RSMV viral factory formation, the localization of the P protein during viral infection was investigated in rice. We probed these sections with a gold-conjugated P-specific antibody to survey P subcellular distribution during the infection. Transmission electron microscopy images revealed that the gold particles were abundantly located in the VFs but sparsely in mature virus particles (Fig. 3c). Since the agMR system had a higher replication efficiency than the gMR system, and VFs are the sites for viral RNA genome replication and transcription, we tested whether the GFP-P granules were involved in agMR replication. *N. benthamiana* leaves were agroinfiltrated to deliver wild-type P, GFP-P, or P-GFP proteins, together with N, L, VSRs, and agMR. At 6 dpi, agMR RNA accumulation was first examined by RT-qPCR. The results showed that the infiltration combination with GFP-P or wild-type P had similar genomic RNA accumulation, but the combination with P-GFP had lower accumulation (Fig. 3d). Western blotting further confirmed that the RFP protein level in wild-type P and GFP-P samples was higher compared with P-GFP samples (Fig. 3e). Next, we evaluated the fluorescence intensity of the agMR second reporter gene RFP. The results showed that the RFP fluorescence intensity was similar under the support of GFP-P or wild-type P, but much less intensity was observed under the support of P-GFP (Fig. 3f).

Since VFs usually contain more than one viral protein, we next investigated the subcellular localization of the

(See figure on next page.)

Fig. 1 Engineering of RSMV anti-genomic and genomic RNA minireplicon (gMR/agMR) system. **a** Schematic representation of the plasmids designed to generate antigenomic-sense and genomic-sense RSMV derivatives and to express the RSMV N, P, L, and VSR proteins in vivo. In the agMR or gMR plasmid, a reporter cassette of antigenomic-sense or genomic-sense RSMV derivative was inserted between the CaMV double 35S promoter (2X35S) and the ribozyme sequence (RZ). Le, leader; tr, trailer; UTR, untranslated region; NPJ/P 5' UTR, intergenic sequences including N 3' UTR, intergenic sequence, and P 5' UTR; Nos, nopaline synthase terminator. **b** GFP foci observation under ultraviolet light (UV). GFP foci in agroinfiltrated leaf tissues were photographed at 12 dpi. Scale bar = 5 cm. **c** Fluorescent microscope images showing the GFP and RFP foci in infiltrated agMR or gMR system leaves at 12 dpi. Scale bar = 20 um. **d** Statistics of the numbers of GFP/RFP foci cells for agMR and gMR system. **e** qRT-PCR analysis of minigenome RNA replication in the agMR and gMR system at 3, 6, and 12 dpi, respectively. *NbPP2A* served as an internal control gene

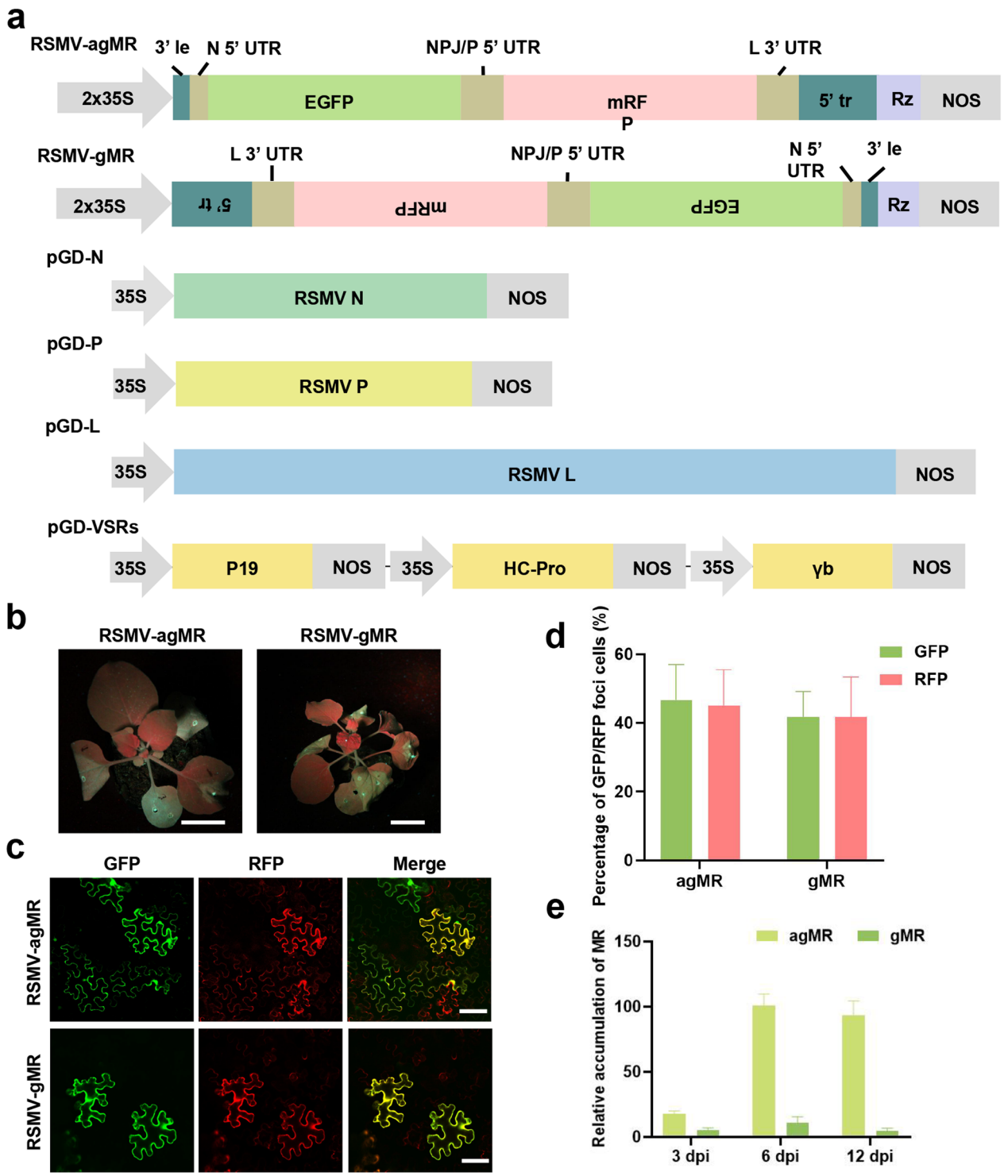

Fig. 1 (See legend on previous page.)

other RSMV proteins. The P3, M, G, and P6 proteins were fused to the N or C termini of GFP and expressed in *N. benthamiana* leaves, respectively. The results showed that both M-GFP, GFP-M, G-CFP, CFP-G, P6-CFP, and CFP-P6 were localized in the cytoplasm or in both the cytoplasm and nucleus (Additional file 1: Figure S2). Interestingly, both GFP-P3 and P3-GFP, especially GFP-P3, formed granules in the cytoplasm.

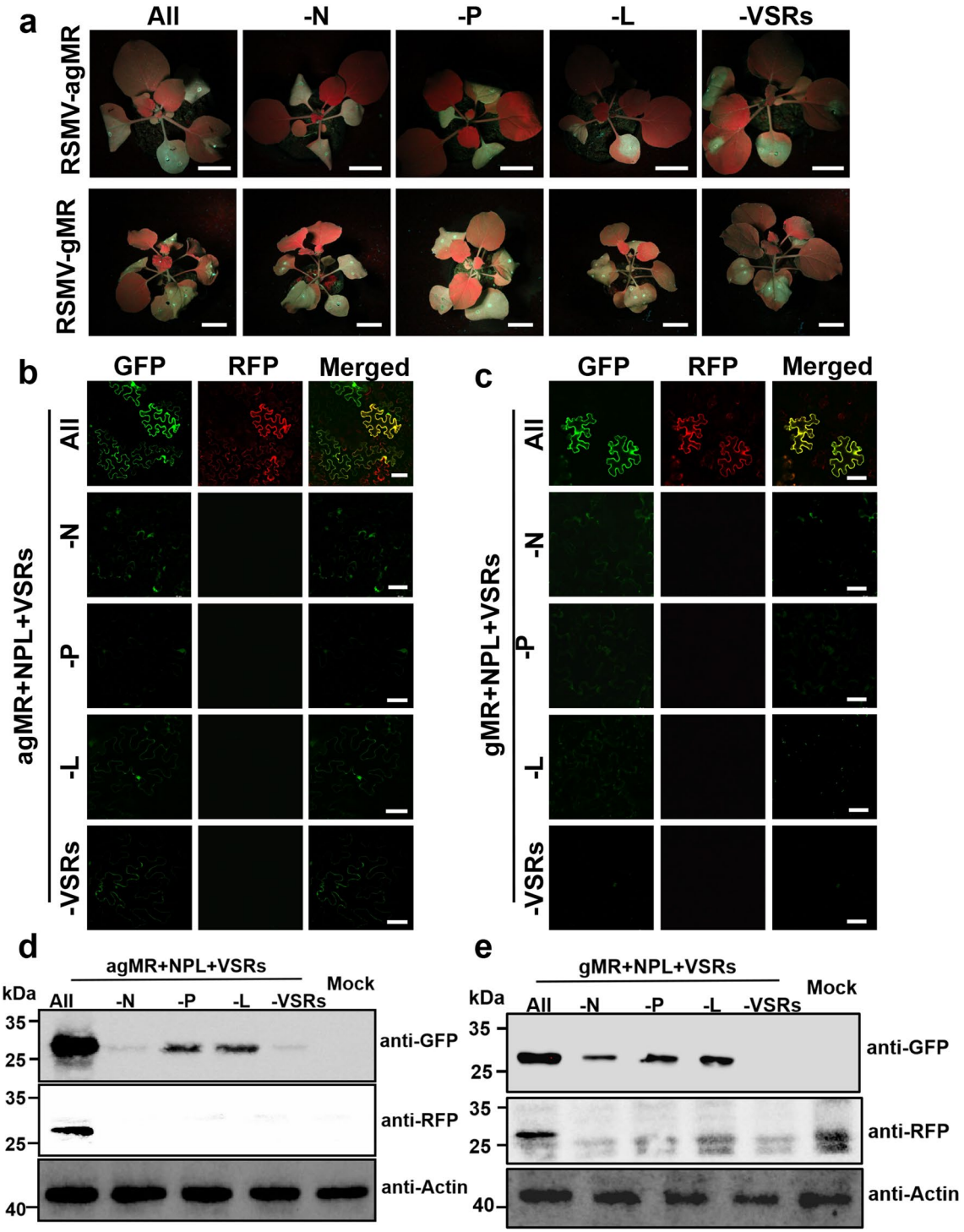

Fig. 2 Requirements of N, P, L, and VSR proteins for agMR/gMR reporter gene expression. **a** GFP foci observation under ultraviolet light (UV). GFP foci in agroinfiltrated leaf tissues were photographed at 12 dpi. Scale bar = 5 cm. **b**, **c** Fluorescent microscope images showing the GFP and RFP foci in infiltrated leaves at 12 dpi. Scale bar = 20 μm. **d**, **e** Western blot analysis showing accumulation of the GFP and RFP proteins in the leaves shown in panels **b** and **c** with mouse antibodies against GFP and RFP. The mock sample was infiltrated with Agrobacterium harboring the empty pGD vector. The mouse antibody against actin was used for protein loading controls

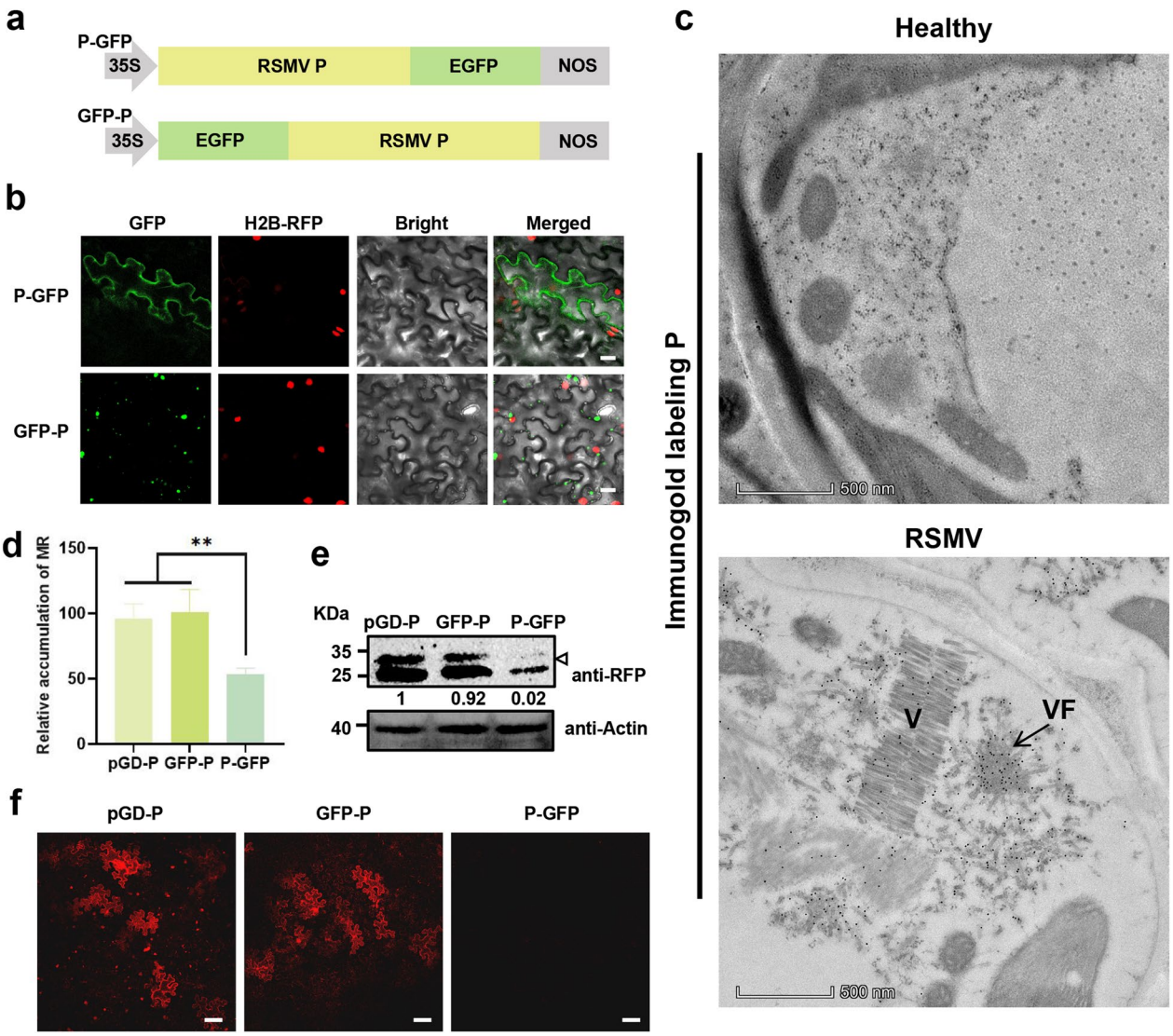

Fig. 3 RSMV GFP-P informs VF-like granules and is functional for agMR replication. **a** Schematic diagram of pGD vectors for the expression of P-GFP and GFP-P. **b** Subcellular distribution of P-GFP and GFP-P in agroinfiltrated leaves of H2B-RFP transgenic *N. benthamiana* at 55 hpi. Scale bar = 20 μm. **c** Immunosorbent electron microscopy analysis of P subcellular localization patterns in non-infected and RSMV-infected rice leaves cells at 30 dpi. Bar = 500 nm. V, virion; VF, viral factory. **d** qRT-PCR analysis of minigenome RNA replication in the agMR with the combination of pGD-P, GFP-P, or P-GFP, respectively. One-way *t*-test was used for analyses, "**" indicates the highly significant difference between the datas, $P < 0.01$. **e** Western blot analysis showing the accumulation of the RFP proteins in the leaves shown in panel (d) with mouse antibodies against RFP. The accumulation of actin protein was used to standardize the concentration of the RFP protein level, and protein concentration further analyzed by ImageJ. **f** Fluorescent microscope images showing the RFP foci in infiltrated leaves at 6 dpi. Scale bar = 100 μm

Moreover, P3-GFP could also localize in the nucleus. (Additional file 1: Figure S2). We then tested whether P3 affects the infection of RSMV agMR in *N. benthamiana* leaves. All RT-qPCR, Western blotting and confocal fluorescence results showed that the P3 protein did not increase the agMR expression compared with the control (Additional file 1: Figure S3).

The IDR2 of P is responsible for P granules formation and is important for agMR replication

We further analyzed which domain is required for the formation of P granules. PONDR (http://pondr.com) was used for P protein IDR domain prediction. The results suggested that RSMV P contained three potential IDRs, including IDR1 (1–101 aa), IDR2 (239–285 aa), and IDR3 (345–376 aa) (Fig. 4a). We next constructed three

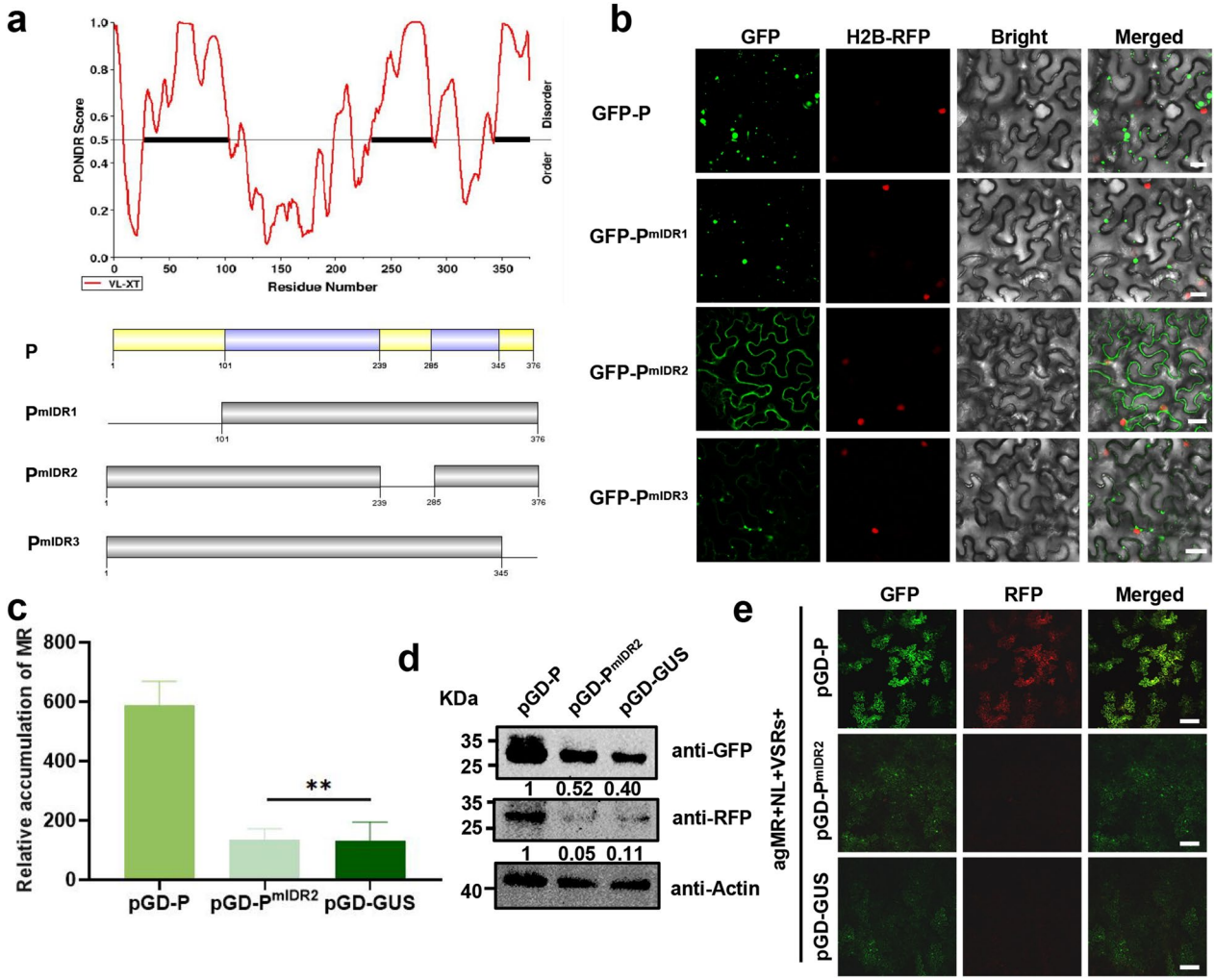

Fig. 4 Identification of RSMV P domains responsible for inclusion body formation. **a** IDR prediction of the RSMV P protein and schematic presentation of deletion mutant designs. Deleted regions of RSMV P are indicated by lines. **b** Subcellular distribution of GFP-fused P and deletion mutants. Images were taken at 55 h after infiltration. Scale bar = 20 μm. **c** qRT-PCR analysis of minigenome RNA replication in the agMR with the combination of pGD-P, pGD-P^{mIDR2}, or pGD-GUS, respectively. **d** Western blot analysis showing accumulation of the GFP and RFP proteins in the leaves shown in panel **c** with mouse antibodies against GFP and RFP. The accumulation of actin protein was used to standardize the concentration of the RFP and GFP protein level, and protein concentration further analyzed by ImageJ. **e** Fluorescent microscope images showing the GFP and RFP foci in infiltrated leaves at 6 dpi. Scale bar = 100 μm

RSMV P mutants named P^{mIDR1}, P^{mIDR2}, and P^{mIDR3}, respectively. These mutants were individually fused with the C-terminus of GFP and expressed in *N. benthamiana* leaves. Subcellular location observation showed that, similar to GFP-P, both GFP-P^{mIDR1} and GFP-P^{mIDR3} formed granules in vivo (Fig. 4b). However, GFP-P^{mIDR2} failed to form granules and was located in the cytoplasm (Fig. 4b).

We next examined whether P^{mIDR2} can support agMR replication. The pGD-P^{mIDR2} construct was infiltrated together with the agMR system. RT-qPCR analysis revealed that the combination with pGD-P^{mIDR2} had a lower agMR RNA accumulation compared with the full-length pGD-P (Fig. 4c). Western blot showed that pGD-P^{mIDR2} had lower levels of GFP and RFP proteins than pGD-P (Fig. 4d). Confocal fluorescence observation showed that, compared with the combination with pGD-P, pGD-P^{mIDR2} could not support the expression of the two reporter genes (Fig. 4e). Collectively, these results demonstrate that IDR2 is essential for RSMV P granules formation and is required for agMR replication.

Discussion

The successful construction of an infectious clone of NSR viruses relies on the exploration and optimization of the mini-replicon reverse genetics system (Ganesan et al. 2013; Fang et al. 2019; Ibrahim et al. 2020; Feng et al. 2021). In this study, we have successfully developed an RSMV mini-replicon system in *N. benthamiana* leaves, laying a solid foundation for the further construction of full-length infectious clones. Previous research has demonstrated that the construction of a Bunyamwera virus (BUNV) infectious clone can be achieved through the transfection of three full-length cDNA clones corresponding to the S, M, and L RNA segments of the virus, respectively. This process does not require the additional transfection of the core protein to assist with transcription (Lowen et al. 2004), indicating that the agRNAs possess the capability to function as mRNA, allowing for translation into BUNV viral proteins prior to encapsidation by the nucleoprotein (N protein). Furthermore, the use of infectious clone of SYNV confirmed that the agRNA derived from the infectious clone can transiently express the N protein. Moreover, the transiently expressed N protein shows a preference for binding to the viral anti-genomic RNA, thereby promoting the replication of the viral gRNA (Ganesan et al. 2013). A residual GFP accumulated in those leaves without the expression of core proteins, which results from direct translation from the GFP ORF at the 5' end of the agRNA transcripts. A similar result was obtained in this study, we found that the GFP reporter gene in the RSMV MR system can be transiently expressed by its 5' cap structure of agRNA, suggesting that the RSMV antisense RNA can transiently express the N protein. Furthermore, research on BYSMV-based MR systems has confirmed that its core component, the P protein, can form mobile inclusions and specifically bind to the N protein, promoting viral replication (Fang et al. 2019). Based on BYSMV MR systems, research has also demonstrated that the phosphorylation and dephosphorylation of the P protein can regulate viral replication and transcription processes (Zhang et al. 2020), showcasing the potential of MR systems in studying viral protein functions. The successful establishment of the MR system for RSMV in this study provides a new approach for studying the functions of RSMV-encoded proteins.

Research has shown that the SYNV infectious clone system based on gRNA had significantly higher infection efficiency than that based on agRNA (Ganesan et al. 2013). The improved infection efficiencies are manifested by a much greater number of primary foci in infiltrated leaves, elevated systemic infection rates, and accelerated disease onset. This indicates that gRNA-based infectious clones have a faster proliferation and replication rate in plants (Ma et al. 2020). On the contrary, in this study, we found that the replication and transcription levels of the gRNA-based RSMV gMR system were lower than those of the agRNA-based RSMV agMR system (Fig. 2). We speculate that this may be due to the fact that gRNA-based infectious clones require a longer time for the formation of the anti-genome during the initial replication steps, causing the injected leaves to wither before all RSMV proteins are translated.

The rhabdovirus P protein serves as the central component of the virus replication complex and recruits the N and L proteins (Nikolic et al. 2019; Ivanov et al. 2011). For SYNV and LNYV, their N and P proteins are individually localized in the nucleus and cytoplasm, respectively. However, when co-expressed in cells, the N and P proteins' localization changes and form punctate aggregates around the nucleus (Jackson et al. 2005; Redinbaugh et al. 2005; Martin et al. 2011). In contrast, the P protein of BYSMV forms inclusion bodies in the cytoplasm, while the N protein is a nuclear-cytoplasmic protein. When the N protein co-expressed with the P protein, the P protein can recruit the N protein into its punctate aggregates (Fang et al. 2019). In this study, the RSMV P protein is also found to form granules similar to the BYSMV P protein, suggesting that it may possess similar properties. RABV can form membraneless spherical regions in the cytoplasm, and these regions contain viral replication complexes (RNPs), indicating that these membraneless spherical regions are the VFs of RABV. Further observation shows that the P protein largely locates in the VFs, indicating that the P protein is a key component of RABV VFs (Nikolic et al. 2017). In this study, we found that the RSMV P protein is abundant in VFs, confirming the conserved function of the P protein in rhabdoviruses. In addition to the conserved structural proteins involved in the composition of viral particles, numerous viruses also encode a variety of smaller non-structural proteins. These non-structural proteins have been found to perform several critical functions, such as evading host immune responses, enhancing viral replication, and aiding in viral movement. Research on positive-stranded RNA viruses shows that various non-structural proteins contribute to the formation of viral inclusion bodies. For example, the human enterovirus PV non-structural protein 2BC induces the formation of membrane vesicles and remodels host membranes (Barco et al. 1995). The dengue virus NS4A protein co-localizes with structural proteins and genomic RNA in inclusion bodies, indicating its involvement (Miller et al. 2007). In plant viruses, the BYSMV P9 protein acts as a 'porin' on mature viral particles, aiding in viral release and replication (Gao et al. 2024). Our study shows that P3

forms granules in vivo, suggesting that P3 may also play an important role in viral infection. A previous report showed that the RSMV P3 protein complements PVX motility, indicating that P3 is a movement protein (Zhou et al. 2019). Moreover, our results showed that a portion of P3-GFP colocalized within the nucleus, underscoring the need for further validation of the P3's function.

Phase separation, especially liquid–liquid phase separation (LLPS), plays a critical role in the assembly of cellular membraneless organelles such as P bodies, stress granules, and the nucleolus. This process concentrates specific molecules, such as proteins and nucleic acids, into liquid-like compartments to fulfill their biological functions. The underlying molecular mechanisms have garnered increased interest due to the important roles of LLPS in various physiological and pathological processes (Darling et al. 2019). VF is a typical membraneless organelle that undergoes phase separation in vivo and plays an important role in viral replication, transcription, and particle assembly. Phase separation is usually triggered by intrinsically disordered regions (IDRs) of proteins (Alberti et al. 2018). The P protein structure of rhabdoviruses is relatively conserved, which contains IDRs, and is crucial for regulating virus replication (Gérard et al. 2009). The P protein of BYSMV contains IDRs and can form phase separation in vivo and in vitro. P protein-mediated LLPS triggers the formation of localized viral protein condensates for optimal virus replication (Fang et al. 2021). Therefore, this study predicted the IDR of RSMV P protein, and the results showed that RSMV P protein has three potential IDRs. Whether or not RSMV P protein can undergo phase separation needs further investigation. Furthermore, P protein of RABV is involved in regulating the formation of Negri bodies (i.e. viral inclusions). The key site for regulating the formation of viral inclusions is located in its second IDR (Nikolic et al. 2017). This study further investigated the effects of the three IDRs on the formation of RSMV P protein granules. The results showed that the IDR2 region is the key location for RSMV P protein to form granules, and it is crucial for virus replication. Whether the unique granules of RSMV P protein are the center of viral inclusions needs further experimental verification.

Conclusions

In conclusion, this study successfully constructed the RSMV mini-replicon systems, laying a solid foundation for further research on the viral protein function, pathogenic mechanism, and full-length infectious clone construction. Additionally, this study explored the function of the RSMV P protein. Subcellular localization experiments revealed that the P protein forms granules in vivo, and the key region for the formation of these granules is the IDR2 region of P. This has been further confirmed to be crucial for MR replication.

Methods

Plant materials

The *N. benthamiana* (laboratory isolate strain) or H2B-RFP transgenic *N. benthamiana* plants used for expression assays were grown at 23℃ with a 12-h day/night regimen.

Plasmid constructs

For the construction of the RSMV agMR system, total RNA was extracted from RSMV-infected plants using Trizol reagent (Vazyme Biotech, Nanjing, China) and used as a template for reverse transcription (RT) to synthesize the full-length cDNA of RSMV with SuperScript III Reverse Transcriptase (Invitrogen, USA). Briefly, the buffer, primer (Reverse-d/R), RNA, and reverse enzyme were mixed and incubated at 50℃ for 30 min to synthesize the cDNA. The full-length cDNA of RSMV antigenomic RNA (12.7-kilobase) was amplified using Phanta Max Super-Fidelity DNA polymerase (Vazyme Biotech, Nanjing China) using primers (Reverse-a/F and Reverse-d/R), and amplified full-length cDNA fragments of expected sizes generated by PCR were purified using a DNA purification kit (Axygen, AP-GX-50, Beijing, China), and sequenced by Sangon Biotechnology. The correction of the RSMV full length cDNA fragments was confirmed with the original RSMV antigenomic sequence, and then the full-length cDNA fragment was engineered into a binary plasmid, pCB301-2×35S-Nos (Wang et al. 2015), to form pCB301-agRSMV. For the construction of the RSMV agMR plasmid, three viral fragments were amplified using pCB301-agRSMV as a template. These fragments included the RSMV leader sequence (le) to the 5' -untranslated region (UTR) of the RSMV N gene sequence (N 5' -UTR), gene junction (GJ) sequences separating the RSMV N and P genes (NPJ/P 5' -UTR), and the 3'- UTR of the RSMV *L* gene (L 3'- UTR) to the RSMV trailer sequence (tr). The reporter gene, enhanced green fluorescent protein (EGFP), was amplified using pCambia1300-GFP (Hajdukiewicz et al. 1994) as a template and substituted for the N protein open reading frame (ORF). The reporter gene, red fluorescent protein (mRFP), was amplified using pGWB454 (Nakagawa et al. 2007) as a template and substituted for the P protein ORF. These fragments were then assembled using overlap PCR in the following order: 3' le-N 5' UTR-EGFP-NPJ/P 5' UTR-mRFP-L 3' UTR-5' le to form the agMR sequence. For the construction of the RSMV gMR plasmid, the plasmid has an identical sequence but in an

inverted orientation compared with the agMR plasmid. The pGD-N, pGD-P, and pGD-L plasmids were generated by inserting the RSMV N, P, and L ORF cDNA sequences into the pGD vector (Goodin et al. 2002). The pGD-VSRs was obtained from a previous study (Fang et al. 2019).

For subcellular localization assays, the N, P, P3, M, G, P6, and P relative mutants were inserted into the pCambia1300-GFP/N or pCambia1300-GFP/C vector, respectively. To evaluate P and P3 function in MR replication, P mutants and P3 sequences were inserted into the pGD vector, respectively. All the primers were listed in Additional file 2: Table S1.

Agroinfiltration infiltration

Recombinant binary plasmids were introduced into *Agrobacterium* (EHA105) by electroporation. Overnight cultures of Agrobacterium cells were resuspended in infiltration buffer (10 mM MES, 10 mM $MgCl_2$, and 100 μM Acetosyringone, pH 5.6). For agMR/gMR expression assays, cell suspensions were adjusted to an A600 of 0.8 and incubated for 2–4 h at room temperature. Before infiltration, pGD-N, pGD-P, pGD-L, pGD-VSRs, and agMR/gMR cultures were mixed at a 1:1:1:1:1 ratio. The mixed cultures were infiltrated into the leaves of four-week-old *N. benthamiana* plants. For subcellular localization assays, Agrobacterium containing different gene constructs encoding the N, P, P3, M, G, P6, and P mutant proteins were diluted to an OD_{600} of 1.2 and infiltrated into H2B-RFP transgenic plant leaves.

Fluorescence observation

For agMR/gMR expression assays, fluorescence in infiltrated leaves was visualized 6–12 days after agroinfiltration using a Leica TCS-SP8 confocal laser scanning microscope. For subcellular localization, visualization was done 55–60 h after agroinfiltration. GFP was excited at 488 nm and emission was captured between 498 nm and 540 nm. RFP were excited at 568 nm and emission was captured between 578 nm and 620 nm.

Real-time quantitative RT-PCR (qRT-PCR)

For the detection of agMR/gMR accumulation, total RNA was extracted from the infiltrated leaves using Total RNA Extraction Reagent (Vazyme Biotech, Nanjing, China) according to the manufacturer's instructions. One-step qRT-PCR reactions were performed by amplifying fragments (spanning GFP and RFP genes, primer pair: qMR-F/R) to detect replication levels using the HiScript II One-Step qRT-PCR SYBR Green kit (Vazyme Biotech, Nanjing, China). Briefly, 250 ng of template RNA, 5×One-Step qRT-PCR SYBR Green kit, 1 μL transcript enzyme, and 10 mM of each primer were mixed together in a total volume of 10 μL, and PCR reactions were run as follows: 15 min at 50℃, 3 min at 96℃, followed by 40 cycles of 10 s at 95℃, and 30 s at 60℃, and 10 min, 72℃. The used primers are listed in Additional file 2: Table S1. All qRT-PCR data were normalized with the *NbPP2A* gene. Three independent biological replicates were performed for statistical analysis.

Western blotting analysis

Proteins were extracted from agroinfiltrated *N. benthamiana* leaves harvested at 2–10 days post-infiltration (dpi) and evaluated by Western blotting. The proteins separated by SDS-PAGE were either stained with Coomassie blue or transferred to nitrocellulose membranes and detected with monoclonal antibodies elicited against GFP (1:5000) (Clontech Laboratories, Mountain View, CA), red fluorescent protein (RFP) (1:2000) (ABclonal, China), and actin (1:5000) (Abmart, USA), followed by goat anti-mouse (1:8000) IgG horseradish peroxidase conjugate, Pierce ECL Plus chemiluminescent substrate, and exposure to X-ray films (Bio-Rad, Japan).

Immunosorbent electron microscopy

For immunoelectron microscopy, rice leaves were pre-fixed with 4% PFA (in 100 mM phosphate buffer, pH 7.0) and 0.1% glutaraldehyde (GA) for 2 h, and then post-fixed with 2% PFA overnight at 4℃. After being treated with 0.1 M glycine for 1 h, the fixed leaves were dehydrated in graded ethanol at 4℃ and embedded in LR-white (GE Healthcare, 14,381-UC). The embedding was polymerized at −20℃ using UV light. 100 nm sections were cut and mounted on single slot nickel grids using a Leica UC7 Ultramicrotome. The sections were then mounted on formal supported nickel single slot grids. Next, the sections were incubated in 100 mM phosphate buffer for 15 min, followed by a 15-min incubation in a blocking buffer (1% BSA [Sigma Aldrich, V900933] in 100 mM phosphate buffer, pH 7.0). For observation of RSMV P using single immunosorbent electron microscopy observation, the sections were incubated with a rabbit antibody specific to RSMV P (1:100, v:v) for 1 h at room temperature. This was followed by a 1-h incubation with a 12-nm gold-conjugated goat-anti-rabbit IgG secondary antibody (Sigma Aldrich, G7402) solution (1:100, v:v).

Statistical analysis

Differences were analyzed using a one-way analysis of variance (ANOVA) with Tukey's honest significant difference (HSD) test for multiple comparisons or a one-way *t*-test for comparisons between two means. A P-value ≤ 0.05 was considered statistically significant.

All analyses were performed using SPSS version 2.0 (SPSS, Inc. Chicago, Illinois, USA).

Abbreviations

agMR	Anti-genome minireplicons
agNC	Anti-genomic nucleocapsids
agRNA	Anti-genomic RNA
BUNV	Bunyamwera virus
BYSMV	Barley yellow striate mosaic virus
CaMV	Cauliflower mosaic virus
gMR	Genomic minireplicons
gRNA	Genomic RNA
IDR	Intrinsically disordered regions
L	RNA polymerase
LLPS	Liquid–liquid phase separation
LNYV	Lettuce necrotic yellows virus
MR	Minireplicon
N	Nucleoprotein
NCMV	Northern cereal mosaic virus
NSR	Negative-sense RNA
P	Phosphoprotein
PVX	Potato virus X
RABV	Rabies virus
RNP	Ribonucleoprotein
RSMV	Rice stripe mosaic virus
RSV	Rice stripe virus
RT-qPCR	Reverse transcription- quantitative real-time PCR
SYNV	Sonchus yellow net virus
TSWV	Tomato spotted wilt virus
VSRs	Viral suppressors of RNA silencing protein

Supplementary Information

The online version contains supplementary material available at https://doi.org/10.1186/s42483-025-00317-5.

Additional file 1: Figure S1. Confocal micrographs showing the subcellular localization of the RSMV N protein. **Figure S2.** Confocal micrographs showing the subcellular localization of the RSMV P3, M, G, P6 proteins. **Figure S3.** Effects of P3 in RSMV MR system. a qRT-PCR analysis of minigenome RNA replication in the agMR with the combination of pGD-GUS and pGD-P3, respectively.

Additional file 2: Table S1. Primers used in this study.

Acknowledgements
We thank the late Professor Michael M. Goodin, University of Kentucky, for providing transgenic *N. benthamiana* plants expressing RFP-H2B. We thank Professor Xianbing Wang, China Agricultural University, for providing pGD vector and pGD-VSRs plasmid. We thank Professor Zhenghe Li, Zhejiang University, for providing pCB301 vector.

Author contributions
TZ conceived and designed the experiment. ZW performed most of the research. JZ, XS, SC, and XC carried out some experiments and analyses. ZW and TZ wrote the original manuscript; XY, GZ, and TZ reviewed and finalized the manuscript. All authors read and approved the final manuscript.

Funding
This work was supported by the National Natural Science Foundation of China (32222071, 32072388), the National Key Research and Development Program of China (2022YFA1304400), the Natural Science Foundation of Guangdong Province (2022A1515010770), and the Guangzhou Science and Technology Program (2023B03J1313).

Availability of data and materials
Not applicable.

Declarations

Ethics approval and consent to participate
Not applicable.

Consent for publication
Not applicable.

Competing interests
The authors declare that they have no competing interests.

Received: 16 October 2024 Accepted: 16 January 2025
Published online: 27 March 2025

References

Ahlquist P, French R, Janda M, Loesch-Fries LS. Multicomponent RNA plant virus infection derived from cloned viral cDNA. Proc Natl Acad Sci USA. 1984;81(22):7066–70.
Alberti S, Saha S, Woodruff JB, Franzmann TM, Wang J, Hyman AA. A user's guide for phase separation assays with purified proteins. J Mol Bio. 2018;430:4806–20. https://doi.org/10.1016/j.jmb.2018.06.038.
Barco A, Carrasco L. A human virus protein, poliovirus protein 2BC, induces membrane proliferation and blocks the exocytic pathway in the yeast Saccharomyces cerevisiae. EMBO J. 1995;14:3349–64. https://doi.org/10.1002/j.1460-2075.1995.tb07341.x.
Castel G, Chtéoui M, Caignard G, Préhaud C, Méhouas S, Réal E, et al. Peptides that mimic the amino-terminal end of the rabies virus phosphoprotein have antiviral activity. J Virol. 2009;83:10808–20. https://doi.org/10.1128/jvi.00977-09.
Chenik M, Schnell M, Conzelmann KK, Blondel D. Mapping the interacting domains between the rabies virus polymerase and phosphoprotein. J Virol. 1998;72:1925–30.
Conzelmann KK, Schnell M. Rescue of synthetic genomic RNA analogs of rabies virus by plasmid-encoded proteins. J Virol. 1994;68:713–9. https://doi.org/10.1128/jvi.72.3.1925-1930.1998.
Damayanti TA, Nagano H, Mise K, Furusawa I, Okuno T. Brome mosaic virus defective RNAs generated during infection of barley plants. J Gen Virol. 1999;80(Pt 9):2511–8. https://doi.org/10.1099/0022-1317-80-9-2511.
Darling AL, Zaslavsky BY, Uversky VN. Intrinsic disorder-based emergence in cellular biology: physiological and pathological liquid-liquid phase transitions in cells. Polymers. 2019;11:990. https://doi.org/10.3390/polym11060990.
Dietzgen RG, Kondo H, Goodin MM, Kurath G, Vasilakis N. The family Rhabdoviridae: mono- and bipartite negative-sense RNA viruses with diverse genome organization and common evolutionary origins. Virus Res. 2016;227:158–70. https://doi.org/10.1016/j.virusres.2016.10.010.
Fang X, Yan T, Gao Q, Cao Q, Gao D, Xu W, et al. A cytorhabdovirus phosphoprotein forms mobile inclusions trafficked on the actin/ER network for viral RNA synthesis. J Exp Bot. 2019;70:4049–62. https://doi.org/10.1093/jxb/erz195.
Fang X, Gao Q, Zang Y, Qiao J-H, Gao D, Xu W, et al. Host casein kinase 1-mediated phosphorylation modulates phase separation of a rhabdovirus phosphoprotein and virus infection. Elife. 2021;11:e74884. https://doi.org/10.7554/eLife.74884.
Feng M, Cheng R, Chen M, Guo R, Tao X. Rescue of tomato spotted wilt virus entirely from complementary DNA clones. Proc Natl Acad Sci USA. 2019;117:201910787. https://doi.org/10.1073/pnas.1910787117.
Feng M, Li L, Cheng R, Yuan Y, Dong Y, Chen M, et al. Development of a minireplicon-based reverse-genetics system for rice stripe tenuivirus. J Virol. 2021;95(14):e0058921. https://doi.org/10.1128/jvi.00589-00521.
Ganesan U, Bragg J, Deng M, Marr SK, Lee MY, Qian S, et al. Construction of a sonchus yellow net virus minireplicon: a step toward reverse genetic analysis of plant negative-strand RNA viruses. J Virol. 2013;87:10598–611. https://doi.org/10.1128/JVI.01397-13.
Gao Q, Xu W, Yan T, Fang X, Cao Q, Zhang Z, et al. Rescue of a plant cytorhabdovirus as versatile expression platforms for planthopper and

cereal genomic studies. New Phytol. 2019;223:2120–33. https://doi.org/10.1111/nph.15889.
Gao Q, Zang Y, Qiao J-H, Zhang Z-Y, Wang Y, Han C-G, Wang X-B. The plant rhabdovirus viroporin P9 facilitates insect-mediated virus transmission in barley. Plant Cell. 2024;36(9):3483–97. https://doi.org/10.1093/plcell/koae162.
Gérard FCA, Ribeiro EDA, Leyrat C, Ivanov I, Blondel D, Longhi S, et al. Modular organization of rabies virus phosphoprotein. J Mol Biol. 2009;388(5):978–96. https://doi.org/10.1016/j.jmb.2009.03.061.
Goodin MM, Dietzgen RG, Schichnes D, Ruzin S, Jackson AO. pGD vectors: versatile tools for the expression of green and red fluorescent protein fusions in agroinfiltrated plant leaves. Plant J. 2002;31(3):375–83. https://doi.org/10.1046/j.1365-313x.2002.01360.x.
Hajdukiewicz P, Svab Z, Maliga P. The small, versatile pPZP family of agrobacterium binary vectors for plant transformation. Plant Mol Biol. 1994;25(6):989–94. https://doi.org/10.1007/BF00014672.
Ibrahim A, Dolleweerd C, Drake P, Ma J. Development of a minigenome cassette for Lettuce necrotic yellows virus: a first step in rescuing a plant cytorhabdovirus. PLoS ONE. 2020;15:e0229877. https://doi.org/10.1371/journal.pone.0229877.
Ivanov I, Yabukarski F, Ruigrok RWH, Jamin M. Structural insights into the rhabdovirus transcription/replication complex. Virus Res. 2011;162:126–37. https://doi.org/10.1016/j.virusres.2011.09.025.
Jackson AO, Dietzgen RG, Goodin MM, Bragg JN, Deng M. Biology of plant rhabdoviruses. Annu Rev Phytopathol. 2005;43:623–60. https://doi.org/10.1146/annurev.phyto.43.011205.141136.
Lowen AC, Noonan C, Mclees A, Elliott RM. Efficient bunyavirus rescue from cloned cDNA. Virology. 2004;330:493–500. https://doi.org/10.1016/j.virol.2004.10.009.
Luytjes W, Krystal M, Enami M, Parvin JD, Palese P. Amplification, expression, and packaging of foreign gene by influenza virus. Cell. 1989;59:1107–13. https://doi.org/10.1016/0092-8674(89)90766-6.
Ma X, Li Z. Significantly improved recovery of recombinant sonchus yellow net rhabdovirus by expressing the negative-strand genomic RNA. Viruses. 2020;12(12):1459. https://doi.org/10.3390/v12121459.
Martin K, Dietzgen R, Wang R, Goodin M. Lettuce necrotic yellows cytorhabdovirus protein localization and interaction map, and comparison with nucleorhabdoviruses. J Gen Virol. 2011;93:906–14. https://doi.org/10.1099/vir.0.038034-0.
Mavrakis M, Iseni F, Mazza C, Schoehn G, Ebel C, Gentzel M, et al. Isolation and characterisation of the rabies virus N degrees-P complex produced in insect cells. Virology. 2003;305:406–14. https://doi.org/10.1006/viro.2002.1748.
Miller S, Kastner S, Krijnse-Locker J, Bühler S, Bartenschlager R. The non-structural protein 4A of dengue virus is an integral membrane protein inducing membrane alterations in a 2K-regulated manner. J Biol Chem. 2007;282:8873–82.
Nakagawa T, Suzuki T, Murata S, Nakamura S, Hino T, Maeo K, et al. Improved gateway binary vectors: high-performance vectors for creation of fusion constructs in transgenic analysis of plants. Biotechnol Biochem. 2007;71(8):2095–100.
Nayaka SN, AaK J, Ghosh A, Roy A, Mandal B. Delivery of progeny virus from the infectious clone of cucumber green mottle mosaic virus and quantification of the viral load in different host plants. 3 Biotech. 2023;13:209. https://doi.org/10.1074/jbc.M609919200.
Netherton CL, Wileman T. Virus factories, double membrane vesicles and viroplasm generated in animal cells. Curr Opin Virol. 2011;1:381–7. https://doi.org/10.1016/j.coviro.2011.09.008.
Nikolic J, Le Bars R, Lama Z, Scrima N, Lagaudrière-Gesbert C, Gaudin Y, et al. Negri bodies are viral factories with properties of liquid organelles. Nat Commun. 2017;8:58. https://doi.org/10.1038/s41467-017-00102-9.
Nikolic J, Lagaudrière-Gesbert C, Scrima N, Blondel D, Gaudin Y. Structure and function of negri bodies. Adv Exp Med Biol. 2019;1215:111–27. https://doi.org/10.1007/978-3-030-14741-9_6.
Novoa RR, Calderita G, Arranz R, Fontana J, Granzow H, Risco C. Virus factories: associations of cell organelles for viral replication and morphogenesis. Biol Cell. 2005;97:147–72. https://doi.org/10.1042/BC20040058.
Pattnaik AK, Wertz GW. Cells that express all five proteins of vesicular stomatitis virus from cloned cDNAs support replication, assembly, and budding of defective interfering particles. Proc Natl Acad SciUSA. 1991;88:1379–83. https://doi.org/10.1073/pnas.88.4.1379.
Redinbaugh MG, Hogenhout SA. Plant rhabdoviruses. World Rhabdoviruses. 2005;292(143):163. https://doi.org/10.1007/3-540-27485-5_7.
Rose JK. Positive strands to the rescue again: a segmented negative-strand RNA virus derived from cloned cDNAs. Proc Natl Acad SciUSA. 1996;93:14998–5000. https://doi.org/10.1073/pnas.93.26.14998.
Schnell MJ, Mebatsion T, Conzelmann KK. Infectious rabies viruses from cloned cDNA. EMBO J. 1994;13(18):4195–203. https://doi.org/10.1002/j.1460-2075.1994.tb06739.x.
Wang Q, Ma X, Qian S, Zhou X, Kai S, Chen X, et al. Rescue of a plant negative-strand rna virus from cloned cdna: insights into enveloped plant virus movement and morphogenesis. PLoS Pathog. 2015;11:e1005223. https://doi.org/10.1371/journal.ppat.1005223.
Wang Z, Chen B, Zhang T, Zhou G, Yang X. Rice stripe mosaic disease: characteristics and control strategies. Front Microbiol. 2021;12:715223. https://doi.org/10.3389/fmicb.2021.715223.
Yang X, Huang J, Liu C, Chen B, Zhang T, Zhou G. Rice stripe mosaic virus, a novel cytorhabdovirus infecting rice via leafhopper transmission. Front Microbiol. 2017a;4(7):2140. https://doi.org/10.3389/fmicb.2016.02140.
Yang X, Zhang T, Chen B, Zhou G. Transmission biology of rice stripe mosaic virus by an efficient insect vector recilia dorsalis (hemiptera: cicadellidae). Front Microbiol. 2017b;11(8):2457. https://doi.org/10.3389/fmicb.2017.02457.
Zhang Z, Qiang G, Xiao-Dong F, Dong G. CCR4, a RNA decay factor, is hijacked by a plant cytorhabdovirus phosphoprotein to facilitate virus replication. Elife. 2020;24(9):e53753. https://doi.org/10.7554/eLife.53753.
Zhou X, Lin W, Sun K, Wang S, Zhou X, Jackson AO, et al. Specificity of plant rhabdovirus cell-to-cell movement. J Virol. 2019;93(15):e00296-e319. https://doi.org/10.1128/JVI.00296-19.